Journal of Power Sources 230 (2013) 277–281

Contents lists available at SciVerse ScienceDirect

Journal of Power Sources

journal homepage: www.elsevier.com/locate/jpowsour

Short communication

Structural and electrochemical properties of single crystalline MoV_2O_8 nanowires for energy storage devices

Muhammad Shahid [a,**], Jingling Liu [b], Zahid Ali [c], Imran Shakir [d,e], Muhammad Farooq Warsi [f,*]

[a] Material Science and Engineering, King Abdullah University of Science and Technology, Thuwal 23955-6900, Saudi Arabia
[b] Department of Chemistry, BK-21 School of Chemical Materials Science, SKKU Advanced Institute of Nanotechnology, Research Institute of Advanced Nanomaterials, Sungkyunkwan University, Suwon 440-746, South Korea
[c] National Institute of Lasers and Optronics, Nilore, Islamabad, Pakistan
[d] BK 21 Physics Research Division, Department of Energy Science, Institute of Basic Science, Sungkyunkwan University, Suwon 440-746, Korea
[e] Department of Sustainable Energy, King Saud University, Riyadh, Saudi Arabia
[f] Department of Chemistry, Baghdad-ul-jadeed Campus, The Islamia University of Bahawalpur-63100, Pakistan

HIGHLIGHTS

- MoV_2O_8 nanowires with diameter ~100 nm were synthesized for the first time using cheap facile solution based route.
- Electrochemical studies revealed that the nanowires exhibited specific capacitance 56 Fg^{-1} at the scan rate of 5 mV s^{-1}.
- The nanowires can be used for fabricating energy storage devices like supercapacitors.

GRAPHICAL ABSTRACT

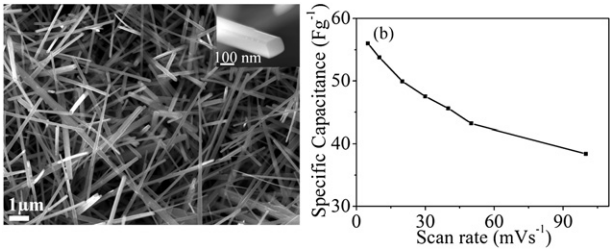

ARTICLE INFO

Article history:
Received 10 November 2012
Received in revised form
4 December 2012
Accepted 6 December 2012
Available online 16 December 2012

Keywords:
Single crystalline
Molybdenum vanadate nanowires
Energy storage devices
Supercapacitors
Electrochemical capacitance

ABSTRACT

We report the synthesis of MoV_2O_8 nanowires of high quality using spin coating followed by the thermal annealing process. Transmission electron microscopy (TEM) reveals the average diameter of synthesized nanowire about 100 nm, and average length ranges from 1 to 5 μm. The TEM analysis further confirms the <001> growth direction of MoV_2O_8 nanowires. The electrochemical properties of synthesized nanowires using cyclic voltammetry show the specific capacitance 56 Fg^{-1} at the scan rate of 5 mV s^{-1} that remains 24 Fg^{-1} at 100 mV s^{-1}. The electrochemical measurements suggest that the MoV_2O_8 nanowires can be used as a material for the future electrochemical capacitors (energy storage devices).

1. Introduction

The synthesis and characterization of one-dimensional (1D) nanostructures (nanowires, nanotubes, nanofibres and nanorods) have gained significant attention due to their novel properties and applications [1–4]. The 1D nanostructures of metal oxides with layered structures have attracted considerable attention due to their potential applications in the field of electronics, actuators, energy storage devices and sensitizers for photolysis of water [5–8]. Nanostructures of metal vanadates are important functional materials, and have different properties depending on their structures and components. Among different vanadates [9,10] molybdenum vanadate (MoV_2O_8) in the form of thin film and bulk powder has

* Corresponding author. Tel.: +92 345 5411391; fax: +92 622 9255474.
** Corresponding author
E-mail addresses: shahid@skku.edu (M. Shahid), farooq.warsi@iub.edu.pk (M.F. Warsi).

0378-7753/$ – see front matter © 2012 Published by Elsevier B.V.
http://dx.doi.org/10.1016/j.jpowsour.2012.12.033

gained considerable interest due to its excellent catalytic, electrical, and magnetic properties [11–13]. As a host for metal ions intercalation, MoV_2O_8 has further advantages due to its layered structure which enhances its ability to intercalate ions in a wide range of sites [14]. It is well known that shape, size, and crystal structure of complex metal oxides can significantly influence the energy density, cycling life, and performance of electrochemical energy devices [15–17].

In the present work we synthesized high-quality single-crystalline MoV_2O_8 nanowires by spin coating the solution directly on a substrate followed by thermal decomposition process without dangerous reagents, harmful solvents, and surfactants. Our results indicate by controlling the structural morphology, MoV_2O_8 showed excellent electrochemical performance which significantly enhanced as compared to the bulk which, in turn, makes them promising candidates for the fabrication of electrochemical and photocatalytic devices.

2. Experimental

All chemicals used in this experiment which include, Ammonium metavanadate (NH_4VO_3) molybdenum water and hydrochloric acid (HCl) were of analytical grade and purchased from Sigma Aldrich. They were used without further purification. In a typical synthesis of MoV_2O_8 nanowires ammonium metavanadate (0.1 mmol) was dissolved in 2 ml of molybdenum water (Mo–water) with continuous stirring. Concentrated HCl (1 ml) was added drop wise for complete dissolution of NH_4VO_3. The resultant yellow solution was used for further experimentation. The precursor solution was spin coated on SiO_2 substrates at 2000 rpm for 30 s which have been ultrasonically cleaned in acetone, alcohol and IPA prior to the deposition. The spin coated substrates were placed into the oven at 550 °C for 2 h.

Electrochemical measurements were carried out using three electrode cell assembly consisting of the glassy carbon as working electrode, Pt wire and Ag/AgCl (satd. KCl) electrodes as counter and reference electrodes respectively, as described in our previous report [18] by using 1 M kC electrolyte solution. Briefly, Galvanostatic charge–discharge studies were performed using a WonATech Potentiostat/galvanostatic instrument (WPG100 South Korea). For the working electrode nanowires were dispersed in ethanol and sonicated for 30 min to achieve good dispersion. From this dispersion 100 μL of the solution was deposited on a glassy carbon electrode and dried at 90 °C. In the final step, nafion solution (5 μl) was coated on the electrode as a binder and dried at room temperature.

3. Results and discussion

3.1. Structural characterization

The FE-SEM analysis (JEOL JSM − 7401F) of the synthesized MoV_2O_8 nanowires was carried out and the results are presented in the Fig. 1(a). The results show that the nanowires having an average diameter of 100 nm and length up to tens of micrometers. X-ray diffraction patterns of the MoV_2O_8 and V_2O_5 nanowires at different temperature are shown in Fig. 1(b). MoV_2O_8 nanowires synthesized at 500 °C have a strong reflection of orthorhombic V_2O_5 and the reflections of MoO_3 are marked with inverted triangle as shown in the Fig. 1(b). However, XRD pattern of the sample synthesized at 550 °C consists of a well-defined diffraction peak of orthorhombic MoV_2O_8 (JCPDS card 74-0050). The oxidation state and elemental composition of the grown nanowires were confirmed by XPS. The XPS spectra of the MoV_2O_8 nanowires in the vanadium 2p, oxygen 1s, and molybdenum 3d regions are shown in Fig. 1(c and d). The main oxygen peak at 530.2 eV was expected for vanadium–oxygen (V–O) bond. The shoulder at higher energy is due to oxygen bond with the surface OH. From Fig. 1(c), the two peaks of vanadium correspond to a doublet V2p3/2 (~517.66 eV) and V2p1/2 (~525.13 eV) in which one is for the 3/2 and the other is for the 1/2 spin-orbit split components. The appearance of a weak band at 521.1 eV is attributed to the X-ray satellite of the O(1s) core level. The comparison of the experimental data with those reported in the literature indicate that the nanowires grown under these conditions are composed of +5 oxidation state of vanadium [19–21]. Fig. 1(d) shows the characteristic doublet Mo3d5/2 at 233.15 eV and Mo3d3/2 at 236.3 eV. The doublet Mo (3d) line is separated by 3.2 eV and their intensity ratio is 2:3. The Mo3d5/2 binding energy of Mo, MoO_2 and MoO_3 is 228.0, 229.4 and 232.6 eV respectively [22]. These results clearly provide evidence that the oxidation state of MoV_2O_8 is +6 (Mo^{6+}).

The nanowires were further characterized by TEM and HR-TEM analysis. The TEM image of the single nanowire is shown in Fig. 2(a). The selective area electron diffraction (SAED) pattern in Fig. 2(b) confirms the single crystalline nature of nanowires. HR-TEM image of a nanowire is shown in Fig. 2(c) in which the lattice fringes are clearly visible. The distance between the neighboring fringes was found to be 4.1 Å which is consistent with the (201) plane of orthorhombic MoV_2O_8. TEM analysis indicates that the growth direction of nanowires is along <001>, resulting in an angle of 60^0 between the zone axes and nanowires. EDS elemental mapping was also carried out to investigate the distribution of the two crystalline materials in the nanowires. The elemental mapping of V, Mo, and O from a nanowire is shown in Fig. 2(d). It was found that elements are homogeneously distributed in the nanowires.

3.2. Electrochemical measurements of nanowires

The electrochemical measurements were conducted in 1 M KCl aqueous solution at room temperature. The rate performance of the nanowires was determined by studying the cyclic voltammograms (CV) at different scanning rates as shown in Fig. 3(a). We observe that the value of current increases slowly with increasing scan rate, showing that specific capacitance of MoV_2O_8 nanowires decreases from 56 to 24 Fg^{-1}. This was mainly because the transfer rate of ions becomes slower with the increase of scan rate due to increase in the resistance of ion diffusion which becomes significant under relatively high scan rate due to the differential depletion of the electrolyte concentration. In addition, the proportion of these inaccessible of the surface area of electrode material also increased with increasing the scan rate, therefore a monotonous decrease in the transfer rate of ions is observed accordingly [23,24].

We further compared the specific capacitance of MoV_2O_8 based supercapacitor with already published V_2O_5 data and found that that the capacitance value of our device is slightly lower than those in the literature [25,26]. However, the specific capacitance of MoV_2O_8 based supercapacitor can be further enhanced by matching the pore sizes and solvated ion sizes of electrolytes, controlling the density of MoV_2O_8 nanowires [27–29]. The variation of specific capacitance with increasing scan rates for nanowires is shown in Fig. 3(b). The long-term chemical and electrochemical stability of the composite was examined by CV at a scan rate of 20 mV s^{-1} over 100 cycles and the corresponding results are presented in Fig. 3(c). The decay capacity was found only 10% even after 100 cycles indicating the excellent stability of the composite material in the energy storage application. We further confirmed the structural and morphological changes of the nanowires after 100 CV cycling. TEM results presented in Fig. 3(d and e) indicate that even after the 100 cycles at 20 mV s^{-1}, the high crystallinity is still maintained.

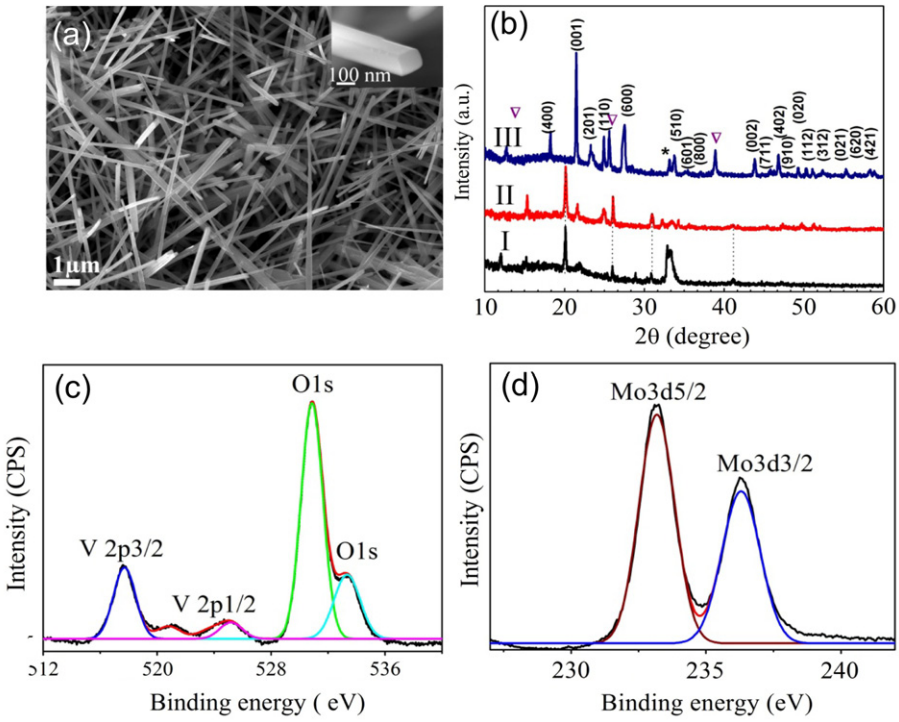

Fig. 1. (a) FE-SEM of nanowires (b) XRD of nanowires at different temperature (I) XRD of V_2O_5,(II) XRD of MoV_2O_8 at 500 °C,(III) XRD of MoV_2O_8 at 550 °C, (▽) MoO_3 and (*) Si substrate (c) XPS of vanadium 2p and oxygen 1s (d) XPS of molybdenum 3d region.

Following the previously reported approach on the layered structure of Mo based oxides; we are able to use the voltammetric sweep rate dependence to determine the charge storage mechanism occurs in MoV_2O_8 nanowires [30–32]. We believe that charge storage occurs in the layered structure of MoV_2O_8 through the following steps:

3.2.1. Step 1

Reaction of cations with electroactive material, followed by a redox reaction [16]. The solid state redox reaction involves electrochemical charge transfer coupled with the insertion of mobile K^+ cations from an electrolyte into the layered structure of MoV_2O_8. The cations are faradaically stored in the layered structure and prohibit the phase transition (structural rearrangement).

3.2.2. Step 2

Electrochemical adsorption of cations on the electroactive material through a charge transfer process. The electrons involved in the non-faradaic charging process are the itinerant conduction band electrons of the MoV_2O_8 nanorods electrode, while the electrons involved in the faradaic processes are transferred to or from valence electron states of the redox cathode or anode reagent. The electrons may, however, arrive in or depart from the conduction band states of the conducting MoV_2O_8 depending on whether the

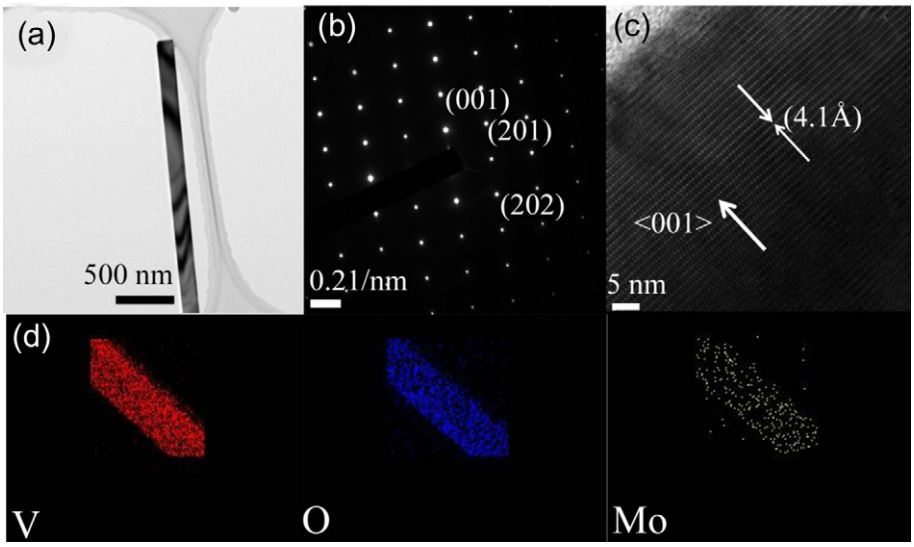

Fig. 2. (a) Low magnification TEM image of nanowires (b) corresponding SAED pattern of individual nanowire recorded along [010] zone axis (c) HR-TEM of nanowire showing high crystallinity (d) TEM Element mapping showing the respective concentrations of vanadium (red circles) oxygen (blue circle) and molybdenum (white circles) in the nanowire. (For interpretation of the references to colour in this figure legend, the reader is referred to the web version of this article.)

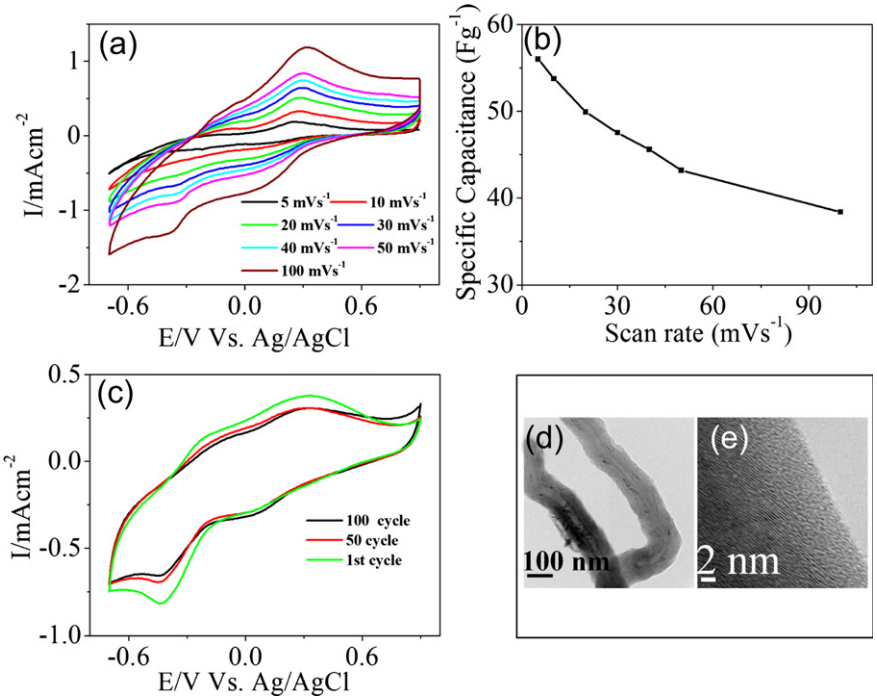

Fig. 3. (a) Cyclic voltammetric plots of MoV_2O_8 nanowires electrode at different scan rates (b) specific capacitances of MoV_2O_8 nanowires electrode calculated from CVs against the number of scans (c) cyclic voltammetry of the first and after 100 cycles (scan rate was 20 mV s^{-1}) (d and e) TEM and HR-TEM of nanowires after electrochemical reaction.

Fermi level in MoV_2O_8 lies below the highest occupied state of the reductant or above the lowest unoccupied state of the oxidant.

3.2.3. Step 3

Intercalation of ions into the van der Waals gaps of the layered structure of MoV_2O_8 [16]. The cations (cathodic reduction) and anions (anodic oxidation) penetrate into the van der Waals gaps between MoV_2O_8 nanowires thus increasing the interlayer distance as shown in Fig. 3(d). The intercalation of ions can increase the charge storage of the MoV_2O_8 nanowires based supercapacitor without compromising charge/discharge kinetics.

Our results are in good agreement with previous studies based on Mo based layered structure materials [30–32] which suggested that pseudocapacitive effects is the main constituent to efficiently store charges in MoV_2O_8 nanowires.

Galvanostatic charge–discharge measurements at different current densities were also carried out to estimate electrochemical properties including specific capacitance, energy, and power. Fig. 4(a) show the charge–discharge curves of nanowires at current density of 1 $mAcm^{-2}$. The nanowires electrodes show a nonlinear charge–discharge curve (inset of Fig. 4(b)), indicating that the nanowires have a pseudocapacitive behavior with a specific capacitance of 56 Fg^{-1}. Specific capacitance is high at low current densities, mainly due to the low ohmic drop, which enables full access of the inner active sites or pores of the electrode. The decrease in capacitance values with increasing current density is mainly because of effective utilization of pseudocapacitive material for ion insertion is limited to the outer surface of electrodes. The electrochemical performance of electrochemical cells was further investigated by the calculating power density and energy density of as-prepared electrodes. The energy density versus power density of nanowires capacitors was plotted on a Ragone chart as shown in Fig. 4(b) after measuring at various charge/discharge currents between −1 and 1 V [29]. The energy density was reduced slowly with increasing power density. The energy density was 17 $Whkg^{-1}$ at a power density of 425 W kg^{-1}, and still remains 5 $Whkg^{-1}$ at a power density of 600 W kg^{-1}, suggesting that MoV_2O_8 nanowires are a promising electrode material for supercapacitor application.

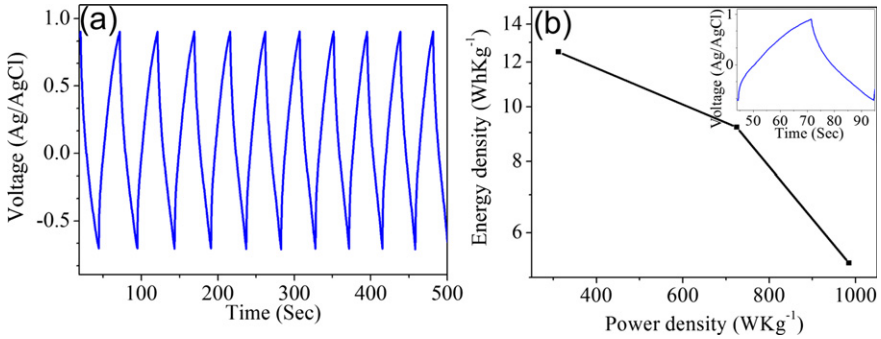

Fig. 4. (a) Galvanostatic charge discharge curves of nanowires at 1mA cm^{-2} (b) Ragone chart of the supercapacitor obtained from discharge curves measured at different constant current densities, the inset shows the zoom-in of galvanostatic charge discharge curves of nanowires at 1 $mAcm^{-2}$.

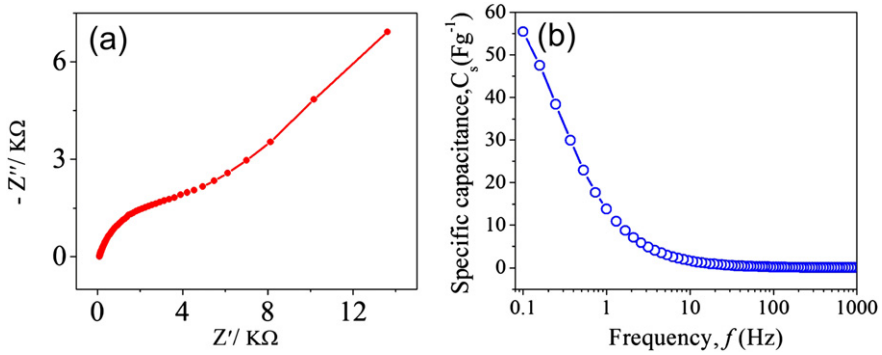

Fig. 5. (a) AC impedance spectra of nanowires (b) Bode plot from impedance spectroscopic analysis showing the specific capacitance as a function of frequency.

The electrochemical properties of the MoV_2O_8 nanowires electrode were also studied by electrochemical impedance spectroscopy (EIS) as shown in Fig. 5(a). The EIS results confirm the excellent electrochemical capacitive properties of the as synthesized MoV_2O_8 nanowire electrode. We further transformed the experimental impedance data to specific capacitance and the results are presented in Fig. 5(b). The specific capacitance of nanowires considerably decreases with increasing the frequency and these results are consistent with decreasing trend with increasing scan rate in CV results [29].

4. Conclusion

In summary, we have synthesized MoV_2O_8 nanowires by spin coated chemical solution deposition method and their electrochemical properties were investigated. CV analysis revealed the pseudocapacitive behavior of the nanowires which was attributed to physisorption of the electrolyte ions on the surface of the MoV_2O_8 nanorods. The cyclic voltammetric analysis for supercapacitor shows that grown nanowires exhibit excellent cyclability with a specific capacitance of 56 Fg^{-1} at the scan rate of 5 mV s^{-1} and remains 24 Fg^{-1} at 100 mV s^{-1}. We believe that the concepts presented in this study will provide a general route for designing nanostructured charge storage application.

Acknowledgments

We are thankful to the Korean Ministry of Education, Science and Technology under grants NRF-2010-0029700 (Priority Research Centers Program) and R31-2008-000-10029-0 (World Class University Program). One of the authors (M.F. Warsi) is thankful to The Islamia University of Bahawalpur (Pakistan) and the Higher Education Commission (HEC) of Pakistan.

References

[1] J. Goldberger, R. He, Y. Zhang, S. Lee, H. Yan, H.-J. Choi, P. Yang, Nature 422 (2003) 599–602.
[2] Y. Nakayama, P.J. Pauzauskie, A. Radenovic, R.M. Onorato, R.J. Saykally, J. Liphardt, P. Yang, Nature 447 (2007) 1098–1101.
[3] K. Nomura, H. Ohta, K. Ueda, T. Kamiya, M. Hirano, H. Hosono, Science 300 (2003) 1269–1272.
[4] Q. Li, G. Lu, J. Power Sources 185 (2008) 577–583.
[5] G. Gu, M. Schmid, P.-W. Chiu, A. Minett, J. Fraysse, G.-T. Kim, S. Roth, M. Kozlov, E. Munoz, R.H. Baughman, Nat. Mater. 2 (2003) 316–319.
[6] C.K. Chan, H. Peng, R.D. Twesten, K. Jarausch, X.F. Zhang, Y. Cui, Nano Lett. 7 (2007) 490–495.
[7] T.G. Xu, C. Zhang, X. Shao, K. Wu, Y.F. Zhu, Adv. Funct. Mater. 16 (2006) 1599–1607.
[8] J.-H. Kim, T. Ayalasomayajula, V. Gona, D. Choi, J. Power Sources 183 (2008) 366–369.
[9] S. Patoux, T.J. Richardson, Electrochem. Commun. 9 (2007) 485–491.
[10] A. Liu, M. Ichihara, I. Honma, H. Zhou, Electrochem. Commun. 9 (2007) 1766–1771.
[11] Y.-m. Li, T. Kudo, Solid State Ionics 86–88 (2) (1996) 1295–1299.
[12] F. Duc, S. Gonthier, M. Brunelli, J.C. Trombe, J. Solid State Chem. 179 (2006) 3591–3598.
[13] A.N. Enyashin, V.V. Ivanovskaya, Y.N. Makurin, V.L. Volkov, A.L. Ivanovskii, Chem. Phys. Lett. 392 (2004) 555–560.
[14] A. Tranchant, R. Messina, J. Power Sources 24 (1988) 85–93.
[15] A.-M. Cao, J.-S. Hu, H.-P. Liang, L.-J. Wan, Angew. Chem. Int. Ed. 44 (2005) 4391–4395.
[16] Z. Chen, Y. Qin, D. Weng, Q. Xiao, Y. Peng, X. Wang, H. Li, F. Wei, Y. Lu, Adv. Funct. Mater. 19 (2009) 3420–3426.
[17] T. Brezesinski, J. Wang, S.H. Tolbert, B. Dunn, Nat. Mater. 9 (2010) 146–151.
[18] M. Shahid, J. Liu, I. Shakir, M.F. Warsi, M. Nadeem, Y.-U. Kwon, Electrochim. Acta 85 (2012) 243–247.
[19] Y. Chen, K. Xie, Z. Liu, Appl. Surf. Sci. 126 (1998) 347–351.
[20] H. Ma, S. Zhang, W. Ji, Z. Tao, J. Chen, J. Am. Chem. Soc. 130 (2008) 5361–5367.
[21] H. Zhao, L. Pan, S. Xing, J. Luo, J. Xu, J. Power Sources 222 (2013) 21–31.
[22] S. Mickevičius, V. Bondarenka, S. Grebinskij, H. Tvardauskas, M. Andriulevičius, S. Tamulevičius, S. Kačiulis, Micron 40 (2009) 126–129.
[23] V. Subramanian, H. Zhu, R. Vajtai, P.M. Ajayan, B. Wei, J. Phys. Chem. B 109 (2005) 20207–20214.
[24] Y. Lin, N. Zhao, W. Nie, X. Ji, J. Phys. Chem. C 112 (2008) 16219–16224.
[25] Q.T. Qu, Y. Shi, L.L. Li, W.L. Guo, Y.P. Wu, H.P. Zhang, S.Y. Guan, R. Holze, Electrochem. Commun. 11 (2009) 1325–1328.
[26] Q. Qu, Y. Zhu, X. Gao, Y. Wu, Adv. Energy Mater. 2 (2012) 950–955.
[27] S. Xu, C. Lao, B. Weintraub, Z.L. Wang, J. Mater. Res. 23 (2008) 2072–2077.
[28] J. Bae, M.K. Song, Y.J. Park, J.M. Kim, M. Liu, Z.L. Wang, Angew. Chem. Int. Ed. 50 (2011) 1683–1687.
[29] R.B. Rakhi, W. Chen, D. Cha, H.N. Alshareef, Nano Lett. 12 (2012) 2559–2567.
[30] L.C. Yang, Q.S. Gao, Y. Tang, Y.P. Wu, R. Holze, J. Power Sources 179 (2008) 357–360.
[31] L. Zhou, L. Yang, P. Yuan, J. Zou, Y. Wu, C. Yu, J. Phys. Chem. C 114 (2010) 21868–21872.
[32] L. Yang, L. Liu, Y. Zhu, X. Wang, Y. Wu, J. Mater. Chem. 22 (2012) 13148–13152.